Jasper Rieser · Felix Endress
Alexander Horoschenkoff
Philipp Höfer · Tobias Dickhut
Markus Zimmermann *Editors*

Proceedings of the Munich Symposium on Lightweight Design 2021

Tagungsband zum Münchner Leichtbauseminar 2021

Springer Vieweg

Proceedings of the Munich Symposium on Lightweight Design 2021

Jasper Rieser · Felix Endress
Alexander Horoschenkoff · Philipp Höfer
Tobias Dickhut · Markus Zimmermann
Editors

Proceedings of the Munich Symposium on Lightweight Design 2021

Tagungsband zum Münchner Leichtbauseminar 2021

Springer Vieweg

Editors
Jasper Rieser
TUM School of Engineering and Design,
Laboratory for Product Development
and Lightweight Design
Technical University of Munich
Garching, Germany

Felix Endress
TUM School of Engineering and Design,
Laboratory for Product Development
and Lightweight Design
Technical University of Munich
Garching, Germany

Alexander Horoschenkoff
Munich University of Applied Sciences
München, Germany

Philipp Höfer
Universität der Bundeswehr München
Neubiberg, Germany

Tobias Dickhut
Universität der Bundeswehr München
Neubiberg, Germany

Markus Zimmermann
TUM School of Engineering and Design,
Laboratory for Product Development
and Lightweight Design
Technical University of Munich
Garching, Germany

ISBN 978-3-662-65215-2 ISBN 978-3-662-65216-9 (eBook)
https://doi.org/10.1007/978-3-662-65216-9

Editorial Contact: Alexander Grün
This Springer Vieweg imprint is published by the registered company Springer-Verlag GmbH, DE, part of Springer Nature.
The registered company address is: Heidelberger Platz 3, 14197 Berlin, Germany

Preface

Dear reader,
The first volume of these conference proceedings was published only 1 year ago on occasion of the Munich Symposium on Lightweight Design 2020. It was so well received that we decided to make it from now on an inherent part of all future symposia.

For almost 20 years, the Technical University of Munich, the Universität der Bundeswehr München and the University of Applied Sciences Munich have invited all those interested in lightweight design and its industrial application to the annual Munich Symposium on Lightweight Design. Based in the Munich area, home of many research institutes, start-ups and large companies active in the field of lightweight design, the Symposium has become an established event to strengthen the exchange between science and industrial practice.

After the conference has become more and more popular, last year's symposium 2021 was again a great success. Academic researchers and experts from industry provided valuable insights into their current research activities and discussed technical challenges as well as future directions. More than 20 of these presentations, covering the latest advances in additive manufacturing, structural optimization, and the use of composites in lightweight design, can be found in these proceedings.

Lastly, we wish to thank the team of our publisher Springer Vieweg for the cooperation and their great support throughout the entire publication process.

Best regards

March 2022

Jasper Rieser
Felix Endress
Alexander Horoschenkoff
Philipp Höfer
Tobias Dickhut
Markus Zimmermann

Contents

About the Editors

Jasper Rieser research is about topology optimization methods with a particular focus on the design for additive manufacturing. Currently, he is a research associate at the Laboratory for Product Development and Lightweight Design at the Technical University of Munich (TUM) from which he also obtained his bachelor's and master's degree in mechanical engineering.

Felix Endress is a research associate at the Laboratory for Product Development and Lightweight Design at the Technical University of Munich (TUM). He investigates product development approaches for metal additive manufacturing, with a special focus on optimization and validation of aerospace structures. Previously, he conducted research in the field of Engineering Design at the University of Cambridge and Friedrich-Alexander-Universität Erlangen-Nürnberg. He holds master's degrees in Mechanical Engineering and Engineering Management.

Alexander Horoschenkoff studied mechanical engineering at TUM and received his Ph.D. from the mechanical engineering department. He started his career at the research center of Messerschmitt-Bölkow-Blohm (MBB) in Ottobrunn. Within the research core team of the DaimlerChrysler AG he was responsible for the mechanical technology field. Since 2001 he has been a professor at the Munich University of Applied Sciences, Department of Mechanical Engineering, Automotive and Aeronautics Engineering and head of the CC "Smart Composites".

Philipp Höfer is a full professor at the Institute of Lightweight Engineering within the Department of Aerospace Engineering at the Universität der Bundeswehr München. After obtaining his Ph.D. in the field of material modelling and continuum mechanics, he has gained extensive experience in the development of aircraft structures at Airbus over many years. His research interests include the conceptual, functional and structural design of lightweight structures and the investigation of their static and dynamic characteristics by analysis and test.

Tobias Dickhut is a full professor of Composite Materials and Technical Mechanics at the Institute of Aeronautical Engineering within the Department of Mechanical Engineering at the Universität der Bundeswehr München. After obtaining his Ph.D. in the field of lightweight construction and structures with fibre-reinforced plastics, he has gained extensive experience in the development of space structures at MT Aerospace over many years. His research interests include the scientific engineering research and design with composites, in particular the issues of lightweight (hybrid) force transmission into highly stressed structural components made of composite materials and the development of tank structures for cryogenic media.

Markus Zimmermann research is about the design and optimization of complex mechanical systems, such as automobiles or robots. Before he became a professor at TUM, he spent 12 years at BMW designing vehicles for crash and vehicle dynamics. His academic training is in Mechanical Engineering with degrees from the Technical University of Berlin (Diplom), the University of Michigan (M.S.E.) and MIT (Ph.D.).

Efficient Computation of Spatial Truss Structures for Design Optimization Approaches Using Tube-Shaped Thin-Walled Composite Beams

Michael Jäger(✉) and Sandro Wartzack

Engineering Design, Friedrich-Alexander-Universität Erlangen-Nürnberg, Martensstraße 9, 91058 Erlangen, Germany
jaeger@mfk.fau.de, wartzack@mfk.fau.de

Abstract. Spatial truss structures are a stiff, economical, and effective lightweight design method, especially when using composites instead of isotropic materials for the struts. An efficient computation of these structures is crucial for optimization approaches during the product design process. The most common method for computing spatial truss structures relies on hinged connections with tension/compression-only struts, which ignores the bending and coupling effects of composite beams. However, especially when using asymmetric laminates, these effects are no longer neglectable. Within commercial finite element tools, the computation of large truss structures - which include these effects - is a very time-consuming process. Particularly for slender, thin-walled beams a large number of solid/shell elements is required. In this paper, an analytical solution of the stiffness matrix for a tube-shaped thin-walled composite beam is provided. It is based on the classical laminate plate theory and Timoshenko's exact solution including shear deformation and coupling effects. By using three-dimensional exact Timoshenko beam elements, the number of degrees of freedom can be reduced significantly while coupling effects are maintained. This results in a remarkably lower computation time especially needed for topology optimization. The results are compared to a commercial finite element tool using both solid and shell elements.

Keywords: Lightweight design · Spatial truss structures · Structural optimization · Thin-walled composite beams · Timoshenko beam

J. Rieser et al. (Eds.): *Proceedings of the Munich Symposium on Lightweight Design 2021,* Proceedings, pp. 1–12, 2023. https://doi.org/10.1007/978-3-662-65216-9_1

1 Motivation

Spatial truss structures are a well-established design method with a high potential for lightweight design [1,2], especially when lightweight materials are used and the topology is optimized during the design process. The most common method for computing truss structures uses hinged connections and tension/compression-only struts [3], which is a very fast and efficient computation method when using isotropic materials e.g. aluminium. However when anisotropic materials are used, this method is no longer suitable, due to the coupled mechanical behaviour of the material. Therefore a coupled model needs to be used for analysis of composite beams like the classical laminate plate theory in combination with the finite element method. Although this is a very powerful tool for calculating composites, it is not advisable for optimizing spatial truss structures due to the enormous computing costs. Classical approaches for truss structure optimization, such as the ground structure method [4,5] and more advanced methods like an adaptive 'member adding' scheme [6], rely on a very large number of members to be calculated. Therefore an efficient method for computing a large number of struts needs to be used, such as a thin-walled composite beam provided by Librescu and Song [7]. Using this beam theory, an analytical solution for the stiffness matrix for a tube-shaped thin-walled composite beam will be derived in this paper, suitable for large scale optimization approaches of spatial truss structures.

2 Thin-Walled Composite Beam Theory

Assumptions
Let h be the wall thickness along the beam assumed constant, let l be any characteristic cross-sectional dimension of the beam (i.e. diameter, height or width) and L its length [7]. In order to apply this thin-walled composite beam theory, the struts must be slender and thin-walled

$$h/l \leq 0.1, \qquad\qquad l/L \leq 0.1. \tag{1}$$

A tube-shaped Timoshenko beam and its degrees of freedom (DOFs) at both ends are shown in Fig. 1.

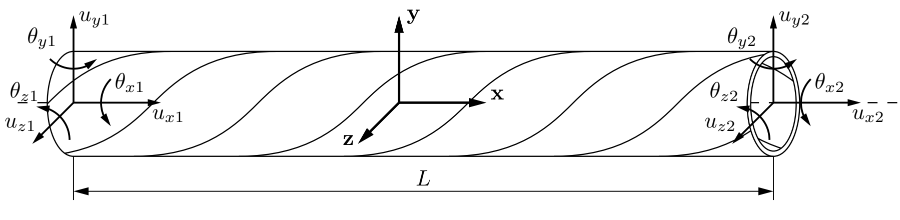

Fig. 1. Timoshenko beam with constant cross section

Additionally, only laminates with a circumferentially uniform stiffness (CUS) configuration [7] (shown in Fig. 2) are considered. Therefore ply layers on opposing sides have to be mirrored

$$\varphi_i(y) = \varphi_i(-y), \qquad \varphi_i(z) = \varphi_i(-z), \tag{2}$$

which is the case for struts manufactured by very common processes like winding, pullwinding, pulltruding or prepreg winding.

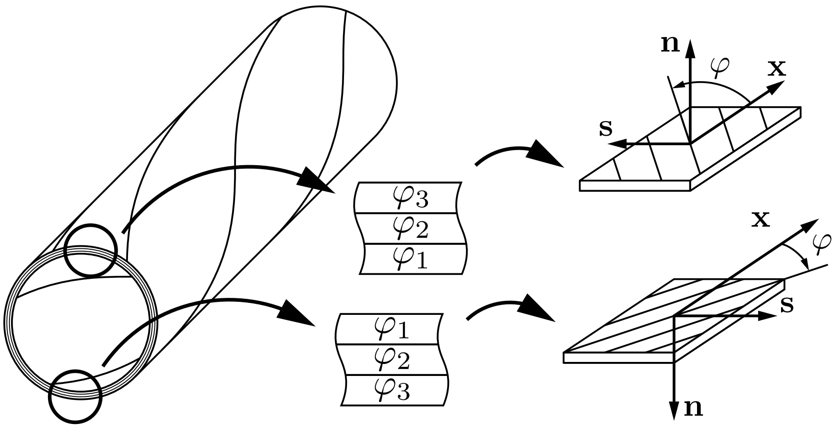

Fig. 2. Circumferentially uniform stiffness (CUS) laminate configuration [7]

Further assumptions for the beam model are, the shape of the cross-section is assumed rigid and remains in its plane, the transverse shear strains are uniform over the beam cross-section [7].

General Beam DAE

Using the symmetry of the CUS laminate configuration, the corresponding cross-sectional stiffness matrix $\mathbf{A}$ for any closed thin-walled beam has the form

$$\mathbf{A} = \begin{bmatrix} a_{11} & 0 & 0 & a_{17} & 0 & 0 \\ 0 & a_{44} & 0 & 0 & a_{34} & 0 \\ 0 & 0 & a_{55} & 0 & 0 & a_{25} \\ a_{17} & 0 & 0 & a_{77} & 0 & 0 \\ 0 & a_{34} & 0 & 0 & a_{33} & 0 \\ 0 & 0 & a_{25} & 0 & 0 & a_{22} \end{bmatrix}. \tag{3}$$

The equivalent properties of a_{ii} for an isotropic beam are $a_{11} \Leftrightarrow EA$, $a_{44} \Leftrightarrow GA_y$, $a_{55} \Leftrightarrow GA_z$, $a_{77} \Leftrightarrow GI_P$, $a_{33} \Leftrightarrow EI_y$, $a_{22} \Leftrightarrow EI_z$ and $a_{ij} \Leftrightarrow 0$, for $i \neq j$. The derivation $\mathbf{A}$ will not be described here, for further information please refer to Sect. 4.4-1 in Librescu and Song [7].

Remark: Compared to Librescu and Song, the cross-sectional stiffness matrix $\mathbf{A}$ is permuted to ensure the following displacement vector $\mathbf{u}(x)$ along the centerline of the beam

$$\mathbf{u}(x) = \left[u_x(x)\; u_y(x)\; u_z(x)\; \theta_x(x)\; \theta_y(x)\; \theta_z(x)\right]^{\mathrm{T}}, \quad \text{for } x \in [0, L], \tag{4}$$

with the DOFs ordered equivalent to common finite element analysis software.

The corresponding differential-algebraic system of equations (DAEs) [7] for a Timoshenko beam with symmetric cross section, CUS laminate configuration and a tube-shaped cross section ($a_{44} = a_{55}$, $a_{22} = a_{33}$, $a_{34} = -a_{25}$) is given as

$$a_{11}\, u_x'' + a_{17}\, \theta_x'' = 0, \tag{5}$$
$$a_{17}\, u_x'' + a_{77}\, \theta_x'' = 0, \tag{6}$$
$$-a_{25}\, \theta_y'' + a_{44}\, (u_y'' + \theta_z') = 0, \tag{7}$$
$$a_{25}\, \theta_z'' + a_{44}\, (u_z'' + \theta_y') = 0, \tag{8}$$
$$a_{22}\, \theta_z'' + a_{25}\, (u_z'' + 2\, \theta_y') - a_{44}\, (u_y' + \theta_z) = 0, \tag{9}$$
$$a_{22}\, \theta_y'' - a_{25}\, (u_y'' + 2\, \theta_z') - a_{44}\, (u_z' + \theta_y) = 0. \tag{10}$$

Remarks: Eqs. (5) and (6) indicate a coupling between extension and twist along the longitudinal axis of the beam for an asymmetric laminate ($a_{17} \neq 0$). Equations (7) to (10) also indicate a coupling between bending about the y- and z-axis for an asymmetric laminate ($a_{25} \neq 0$).

Solution of the DAE

Using the boundary conditions

$$\begin{array}{llll} u_x(0) = u_{x1}, & u_x(L) = u_{x2}, & \theta_x(0) = \theta_{x1}, & \theta_x(L) = \theta_{x2}, \\ u_y(0) = u_{y1}, & u_y(L) = u_{y2}, & \theta_y(0) = \theta_{y1}, & \theta_y(L) = \theta_{y2}, \\ u_z(0) = u_{z1}, & u_z(L) = u_{z2}, & \theta_z(0) = -\theta_{z1}, & \theta_z(L) = -\theta_{z2}, \end{array} \tag{11}$$

the DAE can be solved as follows

$$\mathbf{u}(x) = \mathbf{N}(x)\, \mathbf{u_I}, \tag{12}$$

with $\mathbf{u_I}$ representing the node displacement vector (cf. Fig. 1)

$$\mathbf{u_I} = \left[u_{x1}\; u_{y1}\; u_{z1}\; \theta_{x1}\; \theta_{y1}\; \theta_{z1}\; u_{x2}\; u_{y2}\; u_{z2}\; \theta_{x2}\; \theta_{y2}\; \theta_{z2}\right]^{\mathrm{T}}, \tag{13}$$

and the matrix form functions $\mathbf{N}(x) =$

$$\frac{1}{L\, c_1} \begin{bmatrix} n_{11} & 0 & 0 & 0 & 0 & 0 & n_{17} & 0 & 0 & 0 & 0 & 0 \\ 0 & n_{22} & n_{23} & 0 & n_{25} & n_{26} & 0 & n_{28} & -n_{23} & 0 & n_{211} & n_{212} \\ 0 & -n_{23} & n_{22} & 0 & -n_{26} & n_{25} & 0 & n_{23} & n_{28} & 0 & -n_{212} & n_{211} \\ 0 & 0 & 0 & n_{11} & 0 & 0 & 0 & 0 & 0 & n_{17} & 0 & 0 \\ 0 & 0 & n_{53} & 0 & n_{55} & -n_{23} & 0 & 0 & -n_{53} & 0 & n_{511} & n_{23} \\ 0 & n_{53} & 0 & 0 & -n_{23} & -n_{55} & 0 & -n_{53} & 0 & 0 & n_{23} & -n_{511} \end{bmatrix}. \tag{14}$$

The matrix entries of $\mathbf{N}(x)$ are

$$\begin{aligned}
n_{11} &= \ c_1\,(L-x),\\
n_{17} &= \ c_1\,x,\\
n_{22} &= \ 2\,a_{44}^2\,x^3 - 3\,L\,a_{44}^2\,x^2 - 12\,c_2\,x + L\,c_1,\\
n_{23} &= \ 3\,c_3\,(L-x)\,x,\\
n_{25} &= -c_3\,(2L-x)\,(L-x)\,x,\\
n_{26} &= \ L\,a_{44}^2\,x^3 + (6\,a_{25}^2 - 2\,c_1 + 18\,c_2)\,x^2 - (6\,a_{25}^2 - c_1 + 6\,c_2)\,L\,x,\\
n_{28} &= \ L\,c_1 - n_{22},\\
n_{211} &= -c_3\,(L-x)\,(L+x)\,x,\\
n_{212} &= \ L\,a_{44}^2\,x^3 - (6\,a_{25}^2 + c_1 - 18\,c_2)\,x^2 + 6\,L\,(a_{25}^2 - c_2)\,x,\\
n_{53} &= \ 6\,a_{44}^2\,(L-x)\,x,\\
n_{55} &= \ 3\,L\,a_{44}^2\,x^2 - 4\,(c_1 - 9\,c_2)\,x + L\,c_1,\\
n_{511} &= \ 3\,L\,a_{44}^2 x^2 - (2\,c_1 - 36\,c_2)\,x,
\end{aligned} \tag{15}$$

with

$$c_1 = L^2\,a_{44}^2 + 12\,(a_{22}\,a_{44} - a_{25}^2), \qquad c_2 = a_{22}\,a_{44} - a_{25}^2, \qquad c_3 = 2\,a_{25}\,a_{44}. \tag{16}$$

3 Element Stiffness Matrix

The element stiffness matrix $\mathbf{K}$ for a thin-walled tube-shaped beam is obtained by the strain energy $\mathcal{W}$ [8]. With using the same ansatz functions as the displacement functions $\mathbf{u}(x)$ in Eq. (12), an exact Timoshenko beam element is obtained.

$$\mathcal{W} = \frac{1}{2}\int_0^L \boldsymbol{\varepsilon}^{\mathrm{T}}\,\mathbf{A}\,\boldsymbol{\varepsilon}\,dx = \frac{1}{2}\mathbf{u_I}^{\mathrm{T}}\,\underbrace{\int_0^L \mathbf{B}(x)^{\mathrm{T}}\,\mathbf{A}\,\mathbf{B}(x)\,dx}_{\mathbf{K}}\,\mathbf{u_I}, \tag{17}$$

with $\boldsymbol{\varepsilon}$ being the gradient of the one-dimensional displacement measures represented by $\mathbf{B}(x)\,\mathbf{u_I}$ and $'$ denoting the derivative with respect to x

$$\boldsymbol{\varepsilon} = \begin{bmatrix} u_x' \\ u_y' + \theta_z \\ u_z' + \theta_y \\ \theta_x' \\ \theta_y' \\ \theta_z' \end{bmatrix} = \underbrace{\begin{bmatrix} \mathbf{N}_{1i}' \\ \mathbf{N}_{2i}' + \mathbf{N}_{6i} \\ \mathbf{N}_{3i}' + \mathbf{N}_{5i} \\ \mathbf{N}_{4i}' \\ \mathbf{N}_{5i}' \\ \mathbf{N}_{6i}' \end{bmatrix}}_{\mathbf{B}(x)}\,\mathbf{u_I} = \mathbf{B}(x)\,\mathbf{u_I}. \tag{18}$$

$\mathbf{B}(x)$ can be expressed using the derivative of the form function matrix $\mathbf{N}(x)$ as

$$\mathbf{B} = -\begin{bmatrix} b_{11} & 0 & 0 & 0 & 0 & 0 & -b_{11} & 0 & 0 & 0 & 0 & 0 \\ 0 & b_{22} & b_{23} & 0 & b_{25} & b_{26} & 0 & -b_{22} & -b_{23} & 0 & b_{211} & b_{212} \\ 0 & -b_{23} & b_{22} & 0 & -b_{26} & b_{25} & 0 & b_{23} & -b_{22} & 0 & -b_{212} & b_{211} \\ 0 & 0 & 0 & b_{11} & 0 & 0 & 0 & 0 & 0 & -b_{11} & 0 & 0 \\ 0 & 0 & b_{53} & 0 & b_{55} & -b_{23} & 0 & 0 & -b_{53} & 0 & b_{511} & b_{23} \\ 0 & b_{53} & 0 & 0 & -b_{23} & -b_{55} & 0 & -b_{53} & 0 & 0 & b_{23} & -b_{511} \end{bmatrix}, \quad (19)$$

with

$$\begin{aligned} b_{11} &= c_1, & b_{22} &= 12\,c_2, \\ b_{23} &= -3\,c_3\,(L-2\,x), & b_{25} &= L\,c_3\,(2\,L-3\,x), \\ b_{26} &= 6\,(L-2\,x)\,a_{25}^2 + 6\,L\,c_2, & b_{211} &= L\,c_3\,(L-3\,x), \\ b_{212} &= -6\,(L-2\,x)\,a_{25}^2 + 6\,L\,c_2, & b_{53} &= -6\,a_{44}^2\,(L-2\,x), \\ b_{55} &= -6\,L\,a_{44}^2\,x + 4\,c_1 - 36\,c_2, & b_{511} &= -6\,L\,a_{44}^2\,x + 2\,c_1 - 36\,c_2. \end{aligned} \quad (20)$$

Using $\mathbf{B}(x)$ and $\mathbf{A}$, the beam stiffness matrix $\mathbf{K}$ can be evaluated as

$$\mathbf{K} = \int_0^L \mathbf{B}(x)^{\mathrm{T}}\,\mathbf{A}\,\mathbf{B}(x)\,dx = \frac{1}{L\,c_1}\begin{bmatrix} \mathbf{K_{11}} & \mathbf{K_{12}} & -\mathbf{K_{11}} & -\mathbf{K_{12}}^{\mathrm{T}} \\ & \mathbf{K_{22}} & -\mathbf{K_{12}}^{\mathrm{T}} & \mathbf{K_{24}} \\ & \text{sym.} & \mathbf{K_{11}} & \mathbf{K_{12}}^{\mathrm{T}} \\ & & & \mathbf{K_{22}} \end{bmatrix} \quad (21)$$

with

$$\mathbf{K_{11}} = \begin{bmatrix} k_{11} & 0 & 0 \\ 0 & k_{22} & 0 \\ 0 & 0 & k_{22} \end{bmatrix}, \quad \mathbf{K_{22}} = \begin{bmatrix} k_{44} & 0 & 0 \\ 0 & k_{55} & 0 \\ 0 & 0 & k_{55} \end{bmatrix},$$
$$\mathbf{K_{12}} = \begin{bmatrix} k_{14} & 0 & 0 \\ 0 & k_{25} & k_{26} \\ 0 & -k_{26} & k_{25} \end{bmatrix}, \quad \mathbf{K_{24}} = \begin{bmatrix} -k_{44} & 0 & 0 \\ 0 & k_{511} & k_{512} \\ 0 & -k_{512} & k_{511} \end{bmatrix}, \quad (22)$$

$$\begin{aligned} k_{11} &= a_{11}\,c_1, & k_{55} &= 4\,c_2\,(L^2\,a_{44} + 3\,a_{22}), & k_{22} &= 12\,c_2\,a_{44}, \\ k_{14} &= a_{17}\,c_1, & k_{511} &= 2\,c_2\,(L^2\,a_{44} - 6\,a_{22}), & k_{25} &= -12\,c_2\,a_{25}, \\ k_{44} &= a_{77}\,c_1, & k_{26} &= 6\,c_2\,L\,a_{44}, & k_{512} &= -12\,c_2\,a_{25}\,L. \end{aligned} \quad (23)$$

Remarks: For vanishing coupling effects ($a_{17} = a_{25} = 0$) i.e. a beam with isotropic material, the beam stiffness matrix is equivalent to the one presented by Karadeniz et al. [8].

4 Numerical Examples

In this section, the beam model with the stiffness matrix in Eq. (21) is compared to finite element analyses performed in ANSYS 2021R1 using both solid

(SOLID185) and shell (SHELL181) elements. First, a single tube model with a highly anisotropic laminate is compared, followed by a single tube model with a quasi symmetric laminate. Finally, a comparison for a spacial truss structure with a total number of 64 tubes is drawn. For all examples, the finite element model with solids is considered to be trusted and used as reference.

For all simulations the following material for each unidirectional ply is used. Young's modulus in fibre direction $E_{\parallel} = 134\,639\,\text{MPa}$, Young's modulus perpendicular to the fibre direction $E_{\perp} = 9894\,\text{MPa}$, shear modulus $G_{\perp\parallel} = 4559\,\text{MPa}$ and Poisson's ratio $\nu_{\perp\parallel} = 0.2630$.

Single Beam - Highly Anisotropic Laminate

For the first comparison, a tube with the following dimensions is used: length $L = 1000\,\text{mm}$, inner diameter $d = 26\,\text{mm}$, wall thickness $h = 2\,\text{mm}$. The laminate is made from 4 layers with a thickness of $t_i = 0.5\,\text{mm}$ each and the corresponding ply-angles (inside to outside) are $\varphi_i = [90°, 12°, 30°, 45°]$. The corresponding finite element discretization is shown in Fig. 3.

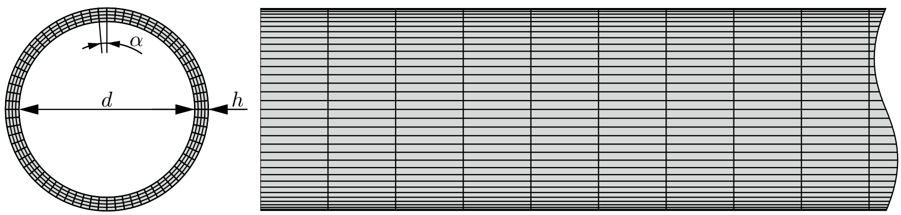

Fig. 3. Finite element discretization of the single tube for solid elements

Along the perimeter, the cross-section is discretized in $\alpha = 5°$ sections resulting in 72 equal elements with an average width of approximately 1.2 mm. Along the length, the tube is discretized in 50 elements with a length of 20 mm each. For the finite element model with solid elements, this gives a total number of 14 400 elements and 56 208 DOFs. The equivalent shell model has 3600 elements and 21 174 DOFs. The FE model is clamped at one end face and load is applied on the opposing end face. For comparison a single beam element based on Eq. (21) is used, the beam is clamped at node one ($u_{x1} = u_{y1} = u_{z1} = \theta_{x1} = \theta_{y1} = \theta_{z1} = 0$) and the load is applied to the second node.

Load Case Tension An axial force of $F_x = 10\,\text{kN}$ is applied, the results are shown in Fig. 4.

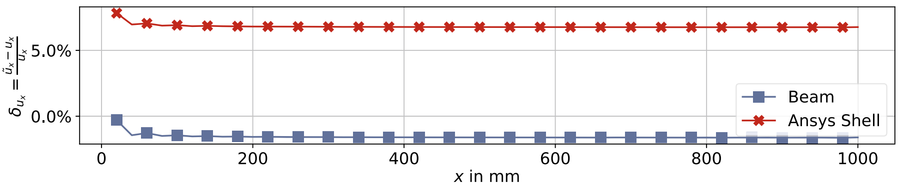

(a) Relative error of displacement $\delta_{u_x} = \frac{\tilde{u}_x - u_x}{u_x}$ relative to the solid model

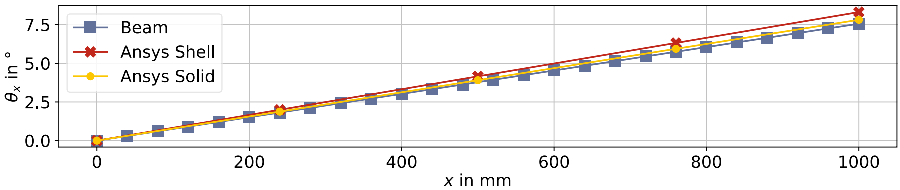

(b) Rotation θ_x caused by coupling of tension and torsion

Fig. 4. Single tube with highly anisotropic laminate under tension $F_x = 10\,\mathrm{kN}$

The displacement u_x and rotation θ_x of the tube under axial tension are well met by the beam model within an error range of less than 2%. The beam model shows a slightly stiffer behaviour than the solid model, but a much smaller deviation than the shell equivalent with an overall less stiff behaviour than the solid model.

Load Case Bending A bending force of $F_y = 50\,\mathrm{N}$ is applied similarly at the end of the tube, the results are shown in Fig. 5.

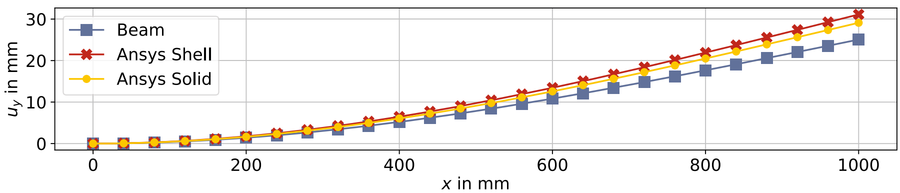

(a) Displacement u_y under bending

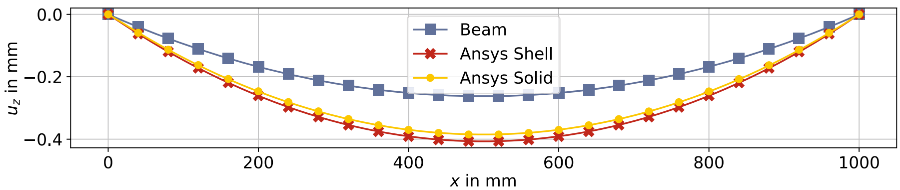

(b) Displacement u_z caused by coupling under bending

Fig. 5. Single tube with highly anisotropic laminate under bending $F_y = 50\,\mathrm{N}$

The beam model still shows a stiffer behaviour than the solid model, resulting in errors of approximately −13.8% in u_y and −31.9% in the coupled u_z direction. The shell model shows a less stiff behaviour than the solid model, with errors of approximately 7% in u_y and 5.6% in the coupled u_z direction.

Single Beam - Slightly Anisotropic Laminate
For this example a more application-oriented laminate made from 6 layers is used. The ply thicknesses are $t_i = [0.2, 0.4, 0.4, 0.2, 0.4, 0.4]$ mm and the corresponding ply-angles (inside to outside) $\varphi_i = [90°, 12°, -12°, 90°, 12°, -12°]$. This results in a quasi symmetric, but slightly anisotropic laminate. All other parameters are retained.

Load Case Tension The displacement u_x and rotation θ_x of the tube under axial tension are shown in Fig. 6. They are very well met by the beam model within an error range of less than 0.6%. In this case the beam model shows a significantly better behaviour in comparison to the shell model with an error above 10% for the displacement and a coupled rotation in the opposite direction.

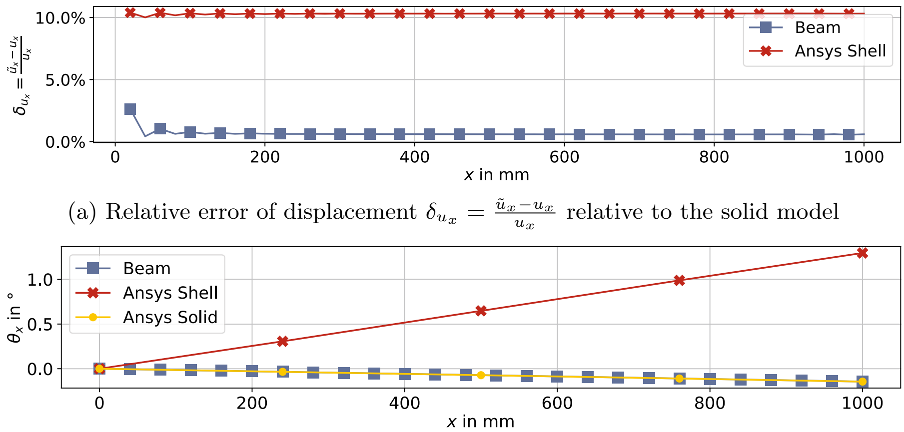

(a) Relative error of displacement $\delta_{u_x} = \frac{\tilde{u}_x - u_x}{u_x}$ relative to the solid model

(b) Rotation θ_x caused by coupling of tension and torsion

Fig. 6. Single tube with slightly anisotropic laminate under tension $F_x = 10$ kN

Load Case Bending For the bending load case, the results are shown in Fig. 7. The beam model shows a very accurate result for u_y with an error under 0.5%. The shell model shows similar results compared to the tension load case, with an relative error around 12% for u_y and a false coupling behaviour for the u_z displacement.

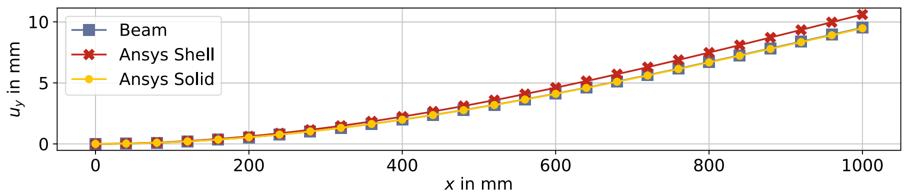

(a) Displacement u_y under bending

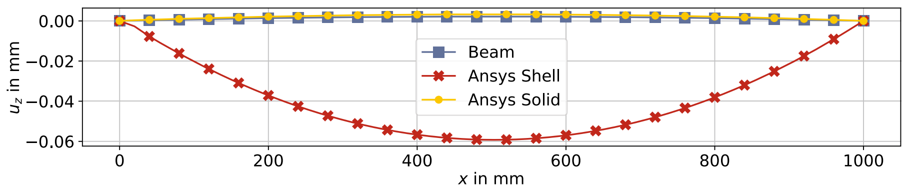

(b) Displacement u_z caused by coupling under bending

Fig. 7. Single tube with slightly anisotropic laminate under bending $F_y = 50\,\mathrm{N}$

Traverse - Slightly Anisotropic Laminate
As final example, a spatial truss structure with 64 tubes made from the slightly anisotropic laminate is compared. The cross section dimensions of the tubes were retained from the examples above, except for the length of each beam. The geometry is shown in Fig. 8, the total size of the traverse is $5000 \times 500 \times 500\,\mathrm{mm}^3$.

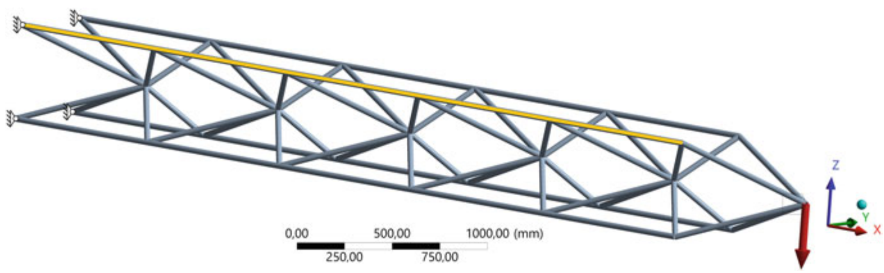

Fig. 8. Traverse model under bending $F_z = -10\,\mathrm{kN}$

The truss structure is clamped at the four nodes on the left side, a bending force of $F_z = -10\,\mathrm{kN}$ is applied at the tip. The displacement is evaluated in Figs. 9 and 10 along the yellow marked path shown in Fig. 8.

The beam model of the truss structure is composed of 64 beam elements with a total number of 156 DOFs. The u_z displacement deviates from the results of the solid model (4 040 376 DOFs) by only 0.6%. In comparison, the shell model's displacement u_z differs by approximately 8% to 9%.

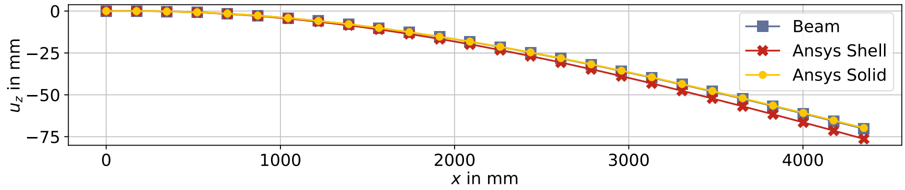

(a) Displacement u_z under bending

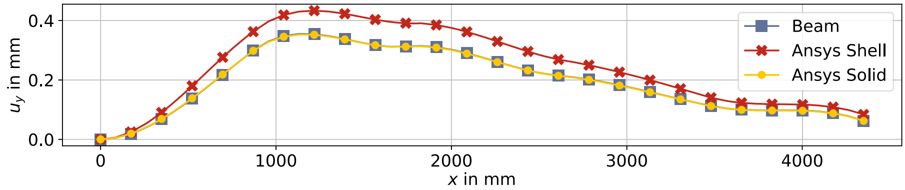

(b) Displacement u_y caused by coupling under bending

Fig. 9. Traverse with slightly anisotropic laminate under bending $F_z = -10\,\mathrm{kN}$

The beam model also mets the coupled u_y displacement very well with an error less than 1%, compared to the shell model (1 047 324 DOFs) with errors up to 35% as shown in Fig. 10b.

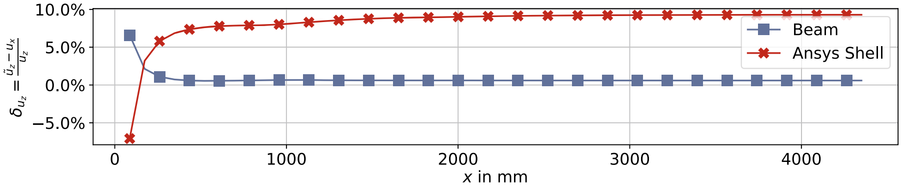

(a) Relative error of displacement $\delta_{u_z} = \frac{\tilde{u}_z - u_z}{u_z}$ relative to the solid model

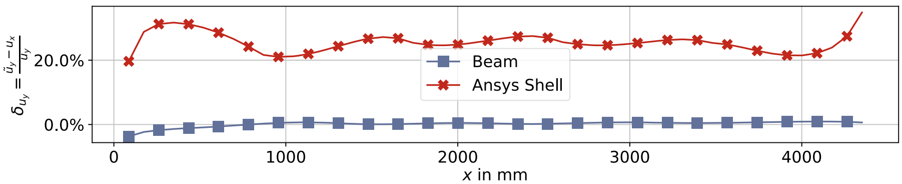

(b) Relative error of displacement $\delta_{u_y} = \frac{\tilde{u}_y - u_y}{u_y}$ relative to the solid model

Fig. 10. Relative error of displacement for a traverse with slightly anisotropic laminate under bending $F_z = -10\,\mathrm{kN}$

Comparing the computation time for this truss, the beam element is orders of magnitude faster. Solving the solid model with Ansys takes 221.02 s (4 CPU cores), preparing the ACP solid model not included (approx. 1200 s). The shell model takes 48.95 s to solve, while the beam model finishes in only 11.86 ms.

5 Conclusion

In the presented contribution the analytical stiffness matrix for tube-shaped thin-walled composite beams has been derived. This allows efficient computing of spatial truss structures while coupling effects within asymmetric laminates are maintained. The number of DOFs can be reduced to a fraction compared to a finite element analysis with solid or shell elements, while errors remain within a reasonable range. Simulations based on highly asymmetric laminates still have potential for further improvement, while truss structures with more application-oriented laminates provide very good results compared to the finite element analysis. Therefore the provided analytical stiffness matrix is well suited for computationally intensive tasks like topology optimization during the product design process of lightweight spatial truss structures made from composites.

Acknowledgments. This Project is supported by the Federal Ministry for Economic Affairs and Energy (BMWi) on the basis of a decision by the German Bundestag.

References

1. H. Pasternak, H.-U. Hoch, and D. Füg. *Stahltragwerke im Industriebau*. EBL-Schweitzer. Ernst, Berlin, 2010. ISBN 9783433600542.
2. D. Klein. *Ein simulationsbasierter Ansatz für die beanspruchungsgerechte Auslegung endlosfaserverstärkter Faserverbundstrukturen*. PhD thesis, Lehrstuhl für Konstruktionstechnik, Friedrich-Alexander-Universität Erlangen-Nürnberg (FAU), VDI Verlag, Düsseldorf, 2017.
3. M. P. Bendsøe and O. Sigmund. *Topology Optimization*. Springer Berlin Heidelberg, Berlin, Heidelberg, 2004. ISBN 978-3-642-07698-5. https://doi.org/10.1007/978-3-662-05086-6.
4. W. S. Dorn, R. E. Gomory, and H. J. Greenberg. Automatic design of optimal structures. In *Journal de Mècanique*, volume 3, pages 25–52, 1964.
5. M. P. Bendsøe, A. Ben-Tal, and J. Zowe. Optimization methods for truss geometry and topology design. *Structural Optimization*, 7(3):141–159, 1994. ISSN 0934-4373. https://doi.org/10.1007/BF01742459.
6. M. Gilbert and A. Tyas. Layout optimization of large-scale pin-jointed frames. *Engineering Computations*, 20:1044–1064, 12 2003. https://doi.org/10.1108/02644400310503017.
7. L. Librescu and O. Song. *Thin-Walled Composite Beams: Theory and Application*, volume 131 of *Solid Mechanics and Its Applications*. Springer-Verlag, Berlin/Heidelberg, 2006. ISBN 1-4020-3457-1. https://doi.org/10.1007/1-4020-4203-5.
8. H. Karadeniz, M. P. Saka, and V. Togan. *Finite Element Analysis of Space Frame Structures*, pages 1–119. Springer London, London, 2013. ISBN 978-1-84996-190-5. https://doi.org/10.1007/978-1-84996-190-5_1.